

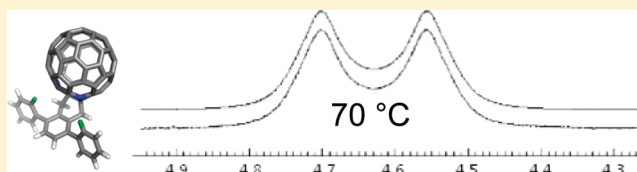
# Probing Intramolecular CH– $\pi$ Interactions in *o*-Quinodimethane Adducts of [60]Fullerene Using Variable Temperature NMR

Ryan P. Kopreski, Jonathan B. Briggs, Weimin Lin, Mikael Jazdyk, and Glen P. Miller\*

Department of Chemistry and Materials Science Program, University of New Hampshire, 23 Academic Way, Durham, New Hampshire 03824, United States

**S** Supporting Information

**ABSTRACT:** Several *o*-quinodimethane adducts of [60]-fullerene were synthesized and their intramolecular aryl CH–fullerene  $\pi$  interactions were studied using variable temperature-NMR (VT-NMR). Evaluation of the rate constants associated with the first-order transition states for cyclohexene boat-to-boat inversions enables quantification of  $\Delta G^\ddagger$  values for each inversion. A comparison between two constitutional isomers, only one of which is capable of intramolecular CH– $\pi$  interactions, provides a lower limit of 0.95 kcal/mol for each aryl CH–fullerene  $\pi$  interaction.



## INTRODUCTION

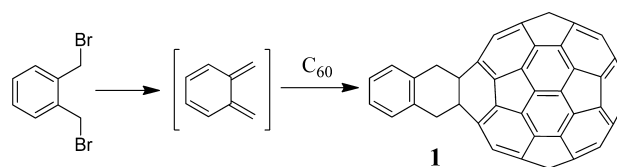
Understanding intermolecular and intramolecular interactions is critical to the rational design of solid-state organic devices including organic photovoltaics and organic light-emitting diodes. These interactions control intramolecular conformations and the relative orientations of molecules in crystalline and thin-film devices and ultimately impact device characteristics. Among the set of interactions at play for polycyclic aromatic hydrocarbons (PAHs), CH– $\pi$  interactions are increasingly recognized as critical to our understanding and prediction of crystal structures.<sup>1</sup> First suggested in 1952 to explain the interaction between benzene and chloroform, CH– $\pi$  interactions are regarded as the weakest of all hydrogen bonds with an estimated enthalpy of approximately 1 kcal/mol.<sup>2,3</sup> Gas-phase studies report the interaction energy of benzene–methane to be 1.03–1.13 kcal/mol.<sup>4</sup> Another example is the benzene dimer which adopts a T-shaped conformation in the solid state.<sup>5</sup> NMR studies of the methyl hydrogens in a number of substituted toluene derivatives in both CCl<sub>4</sub> and benzene solvent reveal chemical shift differences (i.e., greater shielding in benzene solvent than in CCl<sub>4</sub>) as a function of the acidity of the methyl groups.<sup>6</sup> Nakagawa and Fujiwara suggest that this is evidence for CH– $\pi$  interactions between the methyl hydrogens and benzene. In these and other traditional CH– $\pi$  interactions, the interacting orbitals are presumably a  $\sigma^*$  orbital of the H-donor and a  $\pi$  orbital of the H-acceptor.

Recently, Nishio and co-workers made a compelling case that fullerenes routinely participate in CH– $\pi$  interactions.<sup>7</sup> From a Cambridge Crystallographic Database survey, they found numerous examples in which the fullerene  $\pi$  system is located within 3 Å of a CH donor. Often, a CH–fullerene distance was observed at or below 2.9 Å, as low as 2.5 Å. For example, Olmstead and co-workers found that ethyl substituents in porphyrin–[60]fullerene complexes preferentially orient in the

crystal structure such that they are within van der Waals distance of the [60]fullerene cage.<sup>8</sup> In this study, we report intramolecular CH– $\pi$  interactions in *o*-quinodimethane (QDM) adducts of [60]fullerene.

Shortly after the discovery<sup>9</sup> and preparative scale-up<sup>10</sup> of [60]fullerene, a number of derivatives were synthesized including Diels–Alder [4 + 2] cycloadducts.<sup>11</sup> Among the Diels–Alder derivatives, one of the earliest prepared was QDM adduct **1** (Scheme 1).<sup>12</sup> The <sup>1</sup>H and <sup>13</sup>C NMR spectra of this

### Scheme 1. Synthesis of [60]Fullerene *o*-Quinodimethane (QDM) Diels–Alder Adduct



compound indicate a time-averaged C<sub>2v</sub> symmetric structure consistent with a [6:6] addend undergoing dynamic ring-inversion (cyclohexene boat-to-boat inversion) about the methylenes. The <sup>1</sup>H NMR spectrum shows a broadened AB spin system centered at 5.03 ppm indicating that “the ring inversion of the cyclohexene ring is slow on the NMR time scale at room temperature.”<sup>12</sup>

Numerous QDM analogs have been reacted with [60]-fullerene in a similar fashion to give a variety of derivatives.<sup>13–18</sup> In most cases, a dynamically broadened AB multiplet is reported for the methylenes attached to the sp<sup>3</sup> hybridized carbons on the fullerene at the site of addition. Several reports include variable temperature <sup>1</sup>H NMR experiments to further

Received: September 16, 2011

Published: January 4, 2012

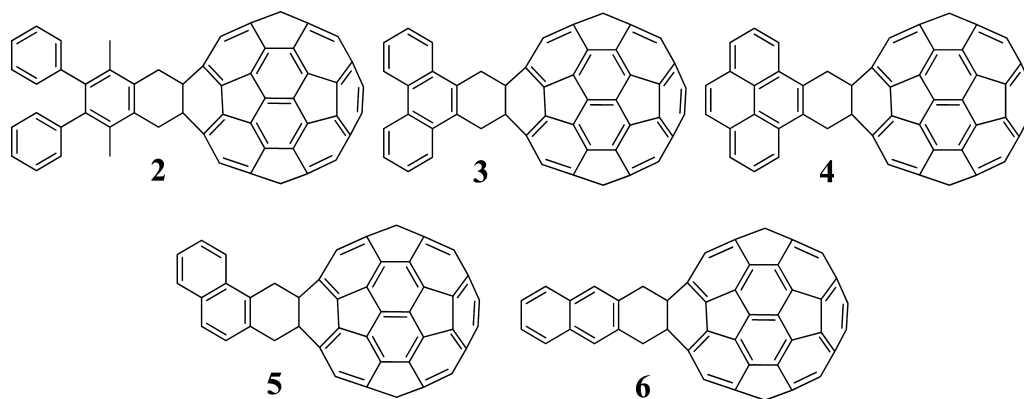


Figure 1. [60]Fullerene–QDM adducts showing dynamically broadened AB multiplets due to exchange of methylene hydrogens.<sup>13–16</sup>

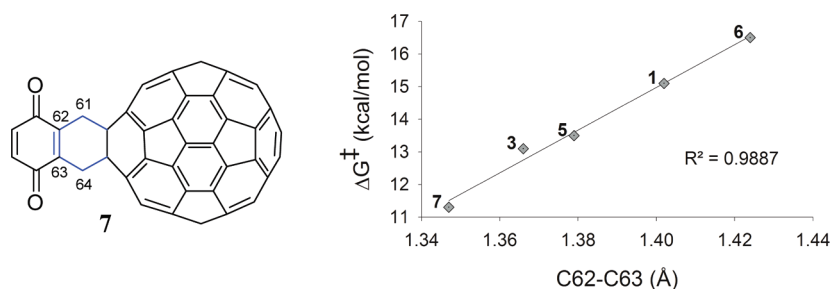


Figure 2. Correlation between PM3-calculated C62–C63 bond lengths in derivatives 1, 3, 5, 6, and 7 and their corresponding barriers to boat-to-boat cyclohexene ring inversion.<sup>18</sup>

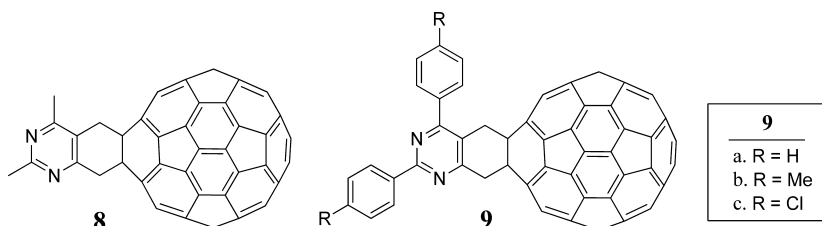


Figure 3. [60]Fullerene–pyrimidine adduct derivatives showing a correlation between aryl substitution and the barrier to inversion of the cyclohexene ring.<sup>19</sup>

study this dynamic phenomenon. Rubin and co-workers carried out the synthesis of 3,6-dimethyl-4,5-diphenyl QDM derivative 2 (Figure 1) which shows coalescence of the AB multiplet at 35 °C.<sup>13</sup> Variable temperature NMR (VT-NMR) experiments were conducted to obtain a <sup>1</sup>H NMR spectrum of the slow-exchange limit which showed a clear AB quartet below –20 °C ( $\Delta\nu_{AB} = 94.8$  Hz,  $J_{AB} = 13.8$  Hz) indicating a free energy of activation,  $\Delta G^\ddagger$ , of 14.6 kcal/mol using eq 1<sup>14</sup> where  $T_c$  is the coalescence temperature in Kelvin,  $\Delta\nu_{AB}$  is the chemical shift difference for the A and B nuclei in Hz,  $J_{AB}$  is the coupling constant in Hz, and  $c$  is a constant dependent on the nature of the exchange, here equal to 9.97.

$$\Delta G_c^\ddagger = 4.57T_c \left[ c + \log \left( \frac{T_c}{\sqrt{\Delta\nu_{AB}^2 + 6J_{AB}^2}} \right) \right] \quad (1)$$

Rubin<sup>13</sup> and others<sup>15</sup> suggest that the relatively high barrier to inversion of the cyclohexene ring is due to the rigidity of the fullerene cage which forces a planar transition state. Nishimura and co-workers synthesized several benzocyclobutene homologues which were reacted with [60]fullerene to generate

derivatives that all demonstrated dynamically broadened AB multiplets.<sup>16</sup> Two such compounds, 3 and 4, are shown in Figure 1. VT-NMR experiments reveal activation barriers for 3 and 4 of 13.1 and 13.2 kcal/mol respectively. In a follow-up study, Nishimura and co-workers additionally examined compounds 5 and 6 (Figure 1).<sup>17</sup> VT-NMR experiments gave free energies of activation of 13.6 and 16.6 kcal/mol, respectively, for these compounds.

Benzoquinone derivative 7 (Figure 2) shows a significantly reduced barrier to boat-to-boat inversion ( $11.3 \pm 0.1$  kcal/mol) of the cyclohexene ring.<sup>18</sup> An interesting correlation was found between the  $\Delta G^\ddagger$  of compounds 1, 3, 5, 6, and 7 and the bond distance between the  $sp^2$  hybridized carbons of the cyclohexene ring (C62–C63) as shown in Figure 2. According to the authors, a smaller bond distance between C62 and C63 allows for slightly greater bond angles for C61–C62–C63 and C62–C63–C64, which in turn relaxes the boat-to-boat inversion constraints at the  $C_{2v}$ -symmetric transition state.

The interest in pyrimidine rings for inclusion in target pharmaceuticals prompted Martin and co-workers to design substituted pyrimidine–fullerene derivatives 8 and 9 as shown in Figure 3.<sup>19</sup> VT-NMR experiments reveal a substituent effect

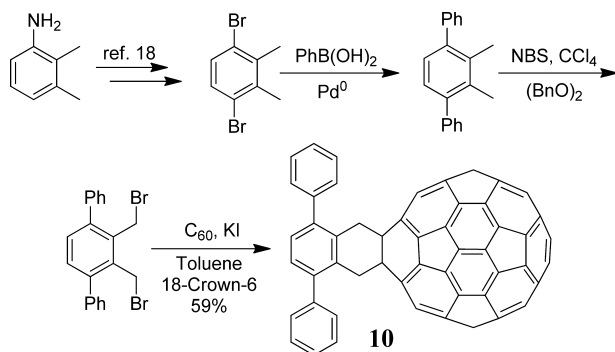
on the barrier to cyclohexene boat-to-boat inversion. Notably, the presence of aryl groups on the pyrimidine ring adds approximately 2 kcal/mol to the barrier ( $\Delta G^\ddagger$ : 8, 15.5, 15.0 kcal/mol; **9a**, 17.0, 16.8 kcal/mol; **9b**, 17.0, 17.2 kcal/mol; **9c**, 17.2, 16.7 kcal/mol). Martin suggests the effect “could be due to high torsional and angular constraints of these structures because of the rigidity of the [fullerene] cage, which is reinforced by the presence of the aryl groups on the pyrimidine ring.”<sup>19</sup> It is unclear, however, how the presence of aryl groups would reinforce the rigidity of the fullerene cage.

Here, we synthesized four new [60]fullerene–QDM derivatives and studied their intramolecular cyclohexene boat-to-boat inversions using VT-NMR. Evaluation of the rate-constants enabled quantification of  $\Delta G^\ddagger$  values for each inversion. Upon the basis of these studies, we conclude that [60]fullerene–QDM derivatives with properly positioned phenyl substituents are prone to engage in favorable aryl CH–fullerene  $\pi$  interactions and we estimate a lower limit of 0.95 kcal/mol for each CH– $\pi$  interaction.

## RESULTS AND DISCUSSION

Synthesis of [60]fullerene–QDM derivative **10** was carried out according to Scheme 2 via 2,3-bis(bromomethyl)-1,4-diphe-

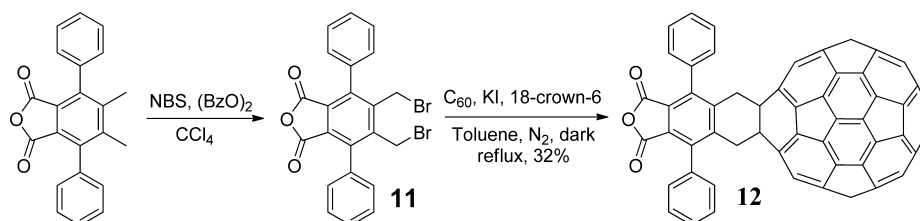
Scheme 2. Synthesis of [60]Fullerene–QDM Derivative **10**



nylbenzene.<sup>20</sup> Unexpectedly, the room temperature <sup>1</sup>H NMR spectrum for **10** shows a sharp AB multiplet for the methylene hydrogens of the cyclohexene ring indicating that boat-to-boat inversion is already in the slow-exchange regime at 25 °C. This feature distinguishes **10** from most [60]fullerene–QDM derivatives like, for example, **1–6**.

VT-NMR studies reveal a strong solvent effect for the coalescence temperature,  $T_c$ , of the exchangeable hydrogens. The  $T_c$  is over 100 °C in toluene-*d*<sub>8</sub> but only 80.5 °C in *o*-dichlorobenzene-*d*<sub>4</sub> as measured by an ethylene glycol chemical shift thermometer. The Gibbs free energy of activation at the coalescence temperature,  $\Delta G_c^\ddagger$ , is calculated to be  $16.6 \pm 0.3$  kcal/mol in *o*-dichlorobenzene-*d*<sub>4</sub> at 80.5 °C using eq 1

Scheme 3. Synthesis of [60]Fullerene–QDM Derivative **12**



(coalescence method) as described above. Structurally similar fullerene adduct **12** (Scheme 3) also shows an unexpectedly high  $T_c$  of 87.3 °C in *o*-dichlorobenzene-*d*<sub>4</sub> indicating a  $\Delta G_c^\ddagger$  equal to  $17.2 \pm 0.3$  kcal/mol. The error ranges associated with  $\Delta G_c^\ddagger$  values for **10** and **12** reflect uncertainties in determining  $T_c$  values using the coalescence method. A side-by-side set of stacked VT-NMR spectra for compounds **10** and **12** are shown in Figure 4.

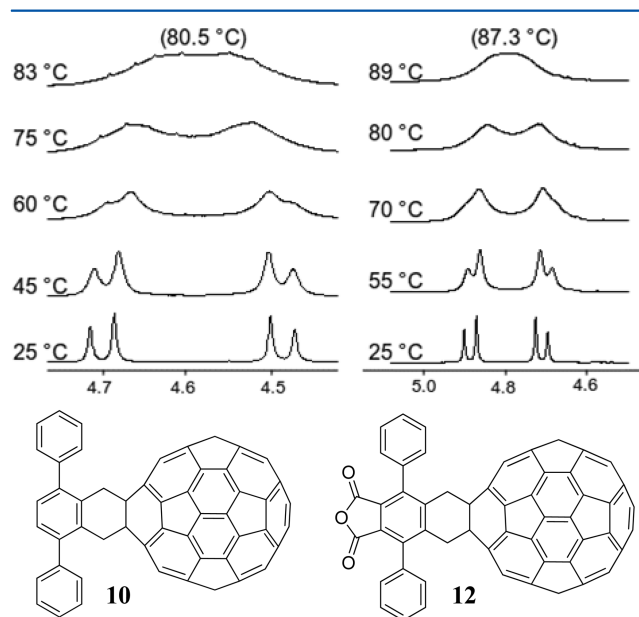
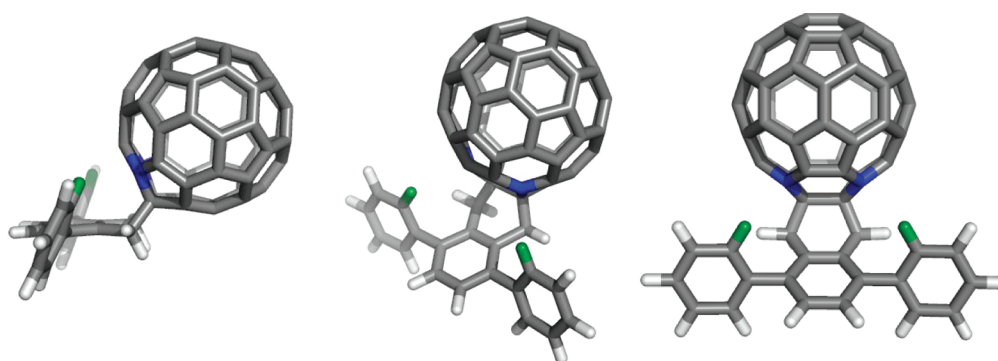
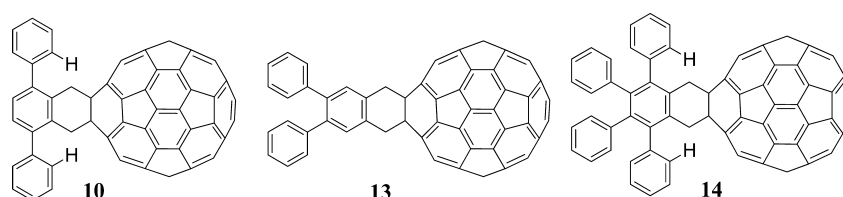


Figure 4. Stacked VT-<sup>1</sup>H NMR plots for compounds **10** and **12** with  $T_c$  values (shown in parentheses) determined using an ethylene glycol chemical shift thermometer.

To understand the high  $T_c$  values for boat-to-boat inversion of compounds **10** and **12**, the ground-state “boat” conformer for compound **10** was optimized using an appropriate force-field (Ghemical, following steepest descent algorithm,  $\Delta E 10^{-4}$  kJ/mol tolerance). The corresponding ground state model indicates that none of the methylene hydrogens of the cyclohexene ring (i.e., C<sub>61</sub>–H<sub>2</sub> and C<sub>64</sub>–H<sub>2</sub>) are properly oriented to engage in meaningful C–H  $\pi$  interactions. However, an *ortho* hydrogen from each phenyl substituent is placed 2.8 Å from the nearest *sp*<sup>2</sup> hybridized fullerene carbon suggesting an aryl CH–fullerene  $\pi$  interaction as shown in Figure 5. We propose that this electrostatic interaction is the major contributing factor to the increased activation energies for the boat-to-boat inversions of **10** and **12** relative to **1**, the unsubstituted QDM–fullerene adduct. To test this proposal, two additional phenyl substituted QDM–fullerene adducts, **13** and **14** (Figure 6), were synthesized. A comparison of diastereomers **10** and **13** allows quantification of the influence



**Figure 5.** Several views of compound **10** depicting the proximity (2.814 Å) of the *ortho* phenyl hydrogens (green) to the nearest fullerene carbons (blue).

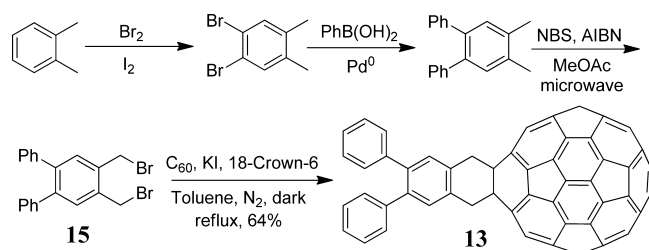


**Figure 6.** Target QDM–fullerene adducts **10**, **13**, and **14**.

of CH– $\pi$  interactions on the energetics of boat-to-boat cyclohexene inversions (*vide infra*).

The syntheses of compounds **13** and **14** were carried out according to Schemes 4 and 5, respectively. It was hypothesized

#### Scheme 4. Synthesis of [60]Fullerene–QDM Derivative **13**

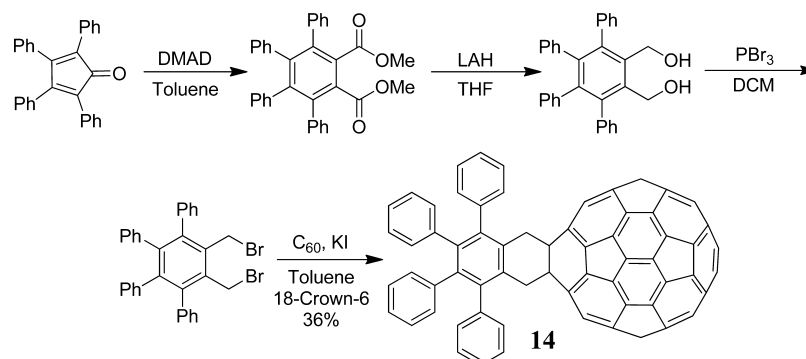


that any difference in  $\Delta G^\ddagger$  values for boat-to-boat inversions of constitutional isomers **10** and **13** would be due to differences in intramolecular CH– $\pi$  interactions. In particular, the phenyl substituents in **13** are too far removed from the fullerene cage to engage in intramolecular CH– $\pi$  interactions. Compound **14** with four successive phenyl substituents adopts a “geared”

conformation as illustrated in Figure 7. This molecular gearing necessitates that only one *ortho* hydrogen atom can engage in a CH– $\pi$  interaction with the fullerene cage at any one time. Thus, we expected a slightly diminished  $T_c$  and  $\Delta G^\ddagger$  value for **14** with respect to **10**.

To obtain accurate Gibbs energies of activation ( $\Delta G^\ddagger$ ) for boat-to-boat inversions of compounds **10**, **13** and **14**, NMR line shapes were simulated at several different temperatures including those where significant line broadening occurred. Thus, VT-NMR studies were conducted for compounds **10**, **13**, and **14** at the approximate temperatures of 25, 40, 55, and 70 °C in *o*-dichlorobenzene- $d_4$ . Because a single solvent was utilized for all three fullerene derivatives, differences in measured  $T_c$  values should be minimally impacted by solvent effects. A low temperature spectrum was collected for each compound to obtain chemical shift values at the slow-exchange limit. For compound **13**, no significant changes in line-shape were observed below –15 °C. Compounds **10** and **14** are already at the slow exchange limit at room temperature. Temperatures of the probe were measured using an ethylene glycol chemical shift thermometer and are reported in Table 1. All dynamically broadened spectra were simulated using Reich's

#### Scheme 5. Synthesis of [60]Fullerene–QDM Derivative **14**



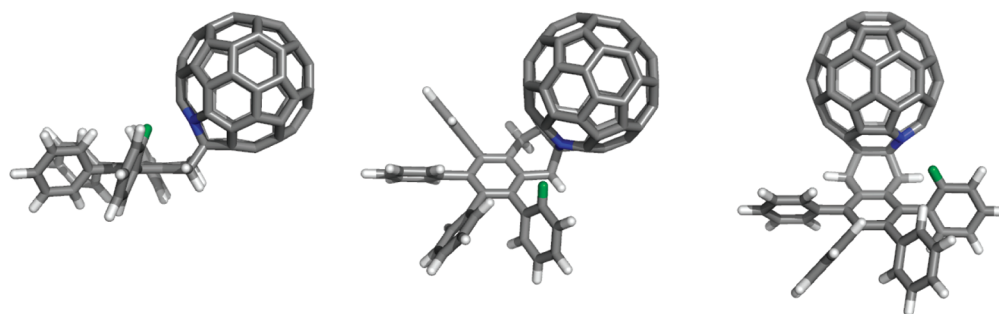


**Figure 7.** Several views of compound **14** (calculated ground state equilibrium geometry, Chemical force-field) depicting the proximity (2.78 Å) of an *ortho* phenyl hydrogen (green) to the nearest fullerene carbon (blue).

**Table 1. Summary of VT-NMR Simulation Data for Compounds 10, 13, and 14<sup>a</sup>**

compound	<i>T</i> (K)	$\Delta\nu_{AB}$ (Hz)	$J_{AB}$ (Hz)	$k$ (s <sup>-1</sup> )	$\Delta G^\ddagger$ (kcal/mol)
10	299.25	104.1	13.9	5.2	16.6
10	313.21	99.2	13.9	12.8	16.8
10	326.87	94.2	13.9	34.9	16.9
<b>10</b>	<b>342.10</b>	<b>91.5</b>	<b>13.9</b>	<b>94.0</b>	<b>17.0</b>
13	299.25	178.7	14.0	66.7	15.0
13	313.21	178.8	14.0	213.8	15.0
<b>13</b>	<b>326.87</b>	<b>174.1</b>	<b>14.0</b>	<b>560.9</b>	<b>15.1</b>
13	342.10	181.6	14.0	1640.9	15.1
14	299.25	49.8	14.0	9.8	16.2
14	313.21	50.6	14.0	19.1	16.5
14	326.87	50.9	14.0	54.3	16.6
<b>14</b>	<b>342.10</b>	<b>51.5</b>	<b>14.0</b>	<b>146.4</b>	<b>16.7</b>

<sup>a</sup>Entries in bold represent data collected nearest the coalescence temperature.

WinDNMR<sup>21</sup> software with all input parameters except temperature taken from the slow-exchange or near slow-exchange limit spectra. Adjustments of spectral amplitudes and rate constants ( $k$ ) were carried out iteratively until the line-shapes matched. Following this,  $\Delta\nu$  was adjusted until the simulated line-shapes overlaid each spectrum. Subsequent iterations on  $k$  and spectral amplitude were carried out if needed until a best fit was achieved.

Simulations for **10**, **13**, and **14** were performed on spectra recorded at approximately 70, 55 and 70 °C, respectively (Figure 8). The Gibbs energies of activation for boat-to-boat inversions ( $\Delta G^\ddagger$ ) were obtained from the Eyring equation (eq 2) where  $R$  is the gas constant,  $T$  is the temperature in Kelvin,  $k$  is the rate-constant obtained from the simulation,  $K$  is the transmission coefficient (equal to 1 in a first order transition),  $k_B$  is Boltzmann's constant, and  $\hbar$  is Planck's constant. The calculated  $\Delta G^\ddagger$  values for **10**, **13** and **14** are summarized in Table 1.

$$\Delta G^\ddagger = RT \left[ \ln \left( \frac{T}{k} \right) + \ln \left( \frac{Kk_B}{\hbar} \right) \right] \quad (2)$$

To use the information collected from Table 1 to approximate the strength of the aryl CH–fullerene  $\pi$  interactions in compounds **10** and **14**, two assumptions are made. First, it is assumed that the steric bulk of the QDM phenyl substituents is approximately the same in **10**, **13** and **14** such that the effects of solvent reorganization can be ignored in the analysis. Second, activation energies are best approximated from line-shape analyses performed at or near  $T_c$  and are

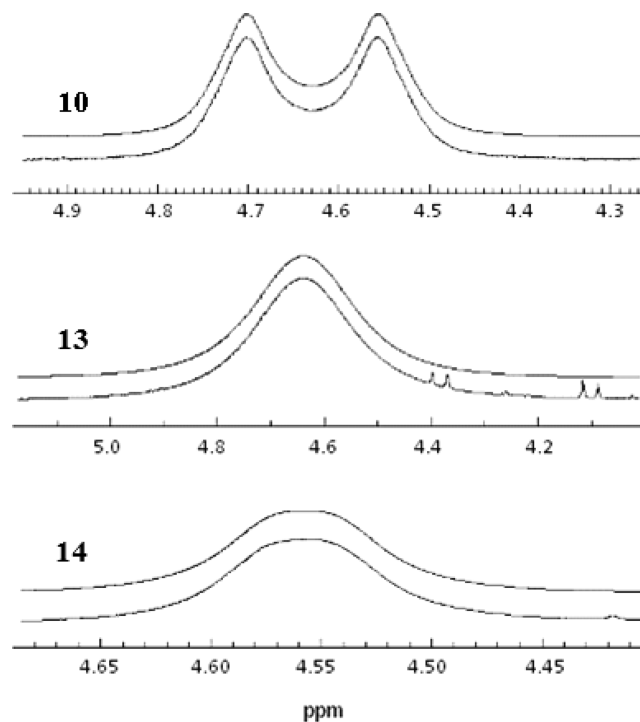


**Figure 8.** Line-shape analyses (simulations above actual spectra in each case) for dynamically broadened methylenes on fullerene adducts **10**, **13**, and **14** recorded at 70, 55 and 70 °C, respectively.

confined to reflect the  $\Delta G^\ddagger$  at the temperature simulated. However, compounds **10** and **14** coalesce at temperatures approximately 15 °C higher than compound **13**. We assumed that this discrepancy would only minimally impact the comparison of  $\Delta G^\ddagger$  values.

With appropriate assumptions in place, the best  $\Delta G^\ddagger$  values for boat-to-boat inversions of **10**, **13** and **14** in *o*-dichlorobenzene-*d*<sub>4</sub> are  $17.0 \pm 0.1$ ,  $15.1 \pm 0.1$ , and  $16.7 \pm 0.1$  kcal/mol, respectively. The  $\Delta G^\ddagger$  values are largest for **10** and **14**, consistent with the inclusion of stabilizing CH– $\pi$  interactions in the ground states of these derivatives. To a first approximation, the difference in  $\Delta G^\ddagger$  values determined for **10** and **13**, 1.9 kcal/mol, can be taken as the total strength of two aryl CH–fullerene  $\pi$  interactions in **10** suggesting that each CH– $\pi$  interaction accounts for approximately 0.95 kcal/mol of stabilization. This value is in agreement with previously measured values for the CH– $\pi$  interaction in the benzene–methane system (1–1.1 kcal/mol).<sup>4</sup> However, our 0.95 kcal/mol estimate must be considered a lower limit. Thus, while the conformation for compound **10** shown in Figure 5 is accessible

at all temperatures, measured  $T_c$  values are for time and conformation averaged species. Compounds **10**, **13** and **14** adopt multiple conformations in *o*-dichlorobenzene- $d_4$  over the time scale of the NMR experiment. For example,  $^1\text{H}$  NMR spectra for compounds **10** and **13** in *o*-dichlorobenzene- $d_4$  show three sharp, resolved signals for the protons of the phenyl substituents (at all temperatures, both above and below  $T_c$ ) indicating rapid, unrestricted rotation of the phenyl rings relative to the NMR time scale (see Supporting Information). If the phenyl substituents were locked into a single conformation (i.e., slow rotation on the NMR time scale) like that depicted in Figure 5, then the corresponding  $^1\text{H}$  NMR spectra would show at least five separate signals for the multiple distinct phenyl protons on **10** and **13**. Since this is not the case in *o*-dichlorobenzene- $d_4$ , we must conclude that our 0.95 kcal/mol value for each aryl CH–fullerene  $\pi$  interaction in **10** is a lower limit.

Interestingly, we observe more than six but far fewer than 20 distinct phenyl proton signals in the room temperature  $^1\text{H}$  NMR spectrum of **14** in *o*-dichlorobenzene- $d_4$  (see Supporting Information), consistent with restricted rotation of the four “gearing” rings, but inconsistent with a conformationally locked ground state. The gearing in **14** prohibits more than one aryl CH–fullerene  $\pi$  interaction at any one time, similar to Martin’s derivative **9**.<sup>19</sup> We conclude that CH– $\pi$  interactions contribute to the overall stabilities of conformation and time averaged species **9**, **10**, **12** and **14**. While none of these molecules is locked into a single conformation, much less one that includes a CH– $\pi$  interaction, the impact of the CH– $\pi$  interactions is sufficient to raise their corresponding  $\Delta G^\ddagger$  values for cyclohexene boat-to-boat inversions relative to [60]fullerene–QDM derivatives like **1–8** and **13** that do not enjoy favorable CH– $\pi$  interactions.

An updated graph similar to the one prepared by Martin and co-workers<sup>18</sup> (Figure 2) supports these conclusions, as illustrated in Figure 9. Newly included compounds **2**, **4**, **8** and **13** all fall along the same trend line as compounds **1**, **3**, **5**, **6**

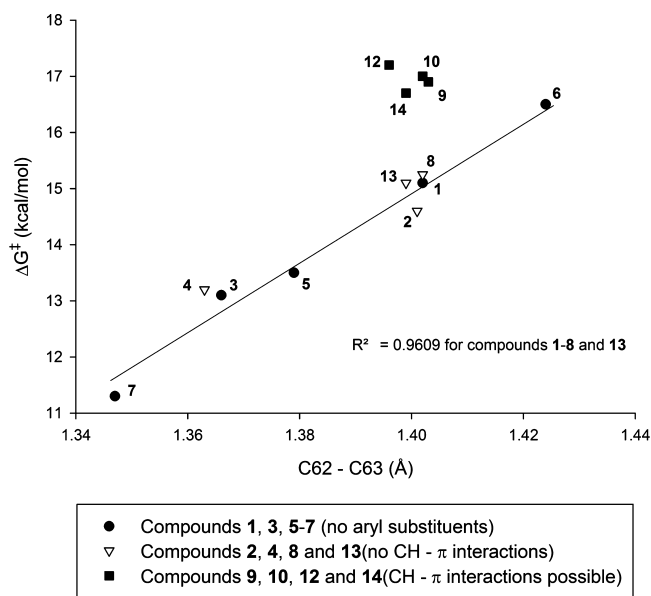


**Figure 9.** Correlation between the C62–C63 bond-lengths in [60]fullerene–QDM derivatives and their corresponding barriers to boat-to-boat cyclohexene ring inversion.

and **7** in the original plot. This validates Martin’s claim that there is a correlation between the PM3 optimized C62–C63 bond lengths for these fullerene derivatives and their corresponding  $\Delta G^\ddagger$  values for cyclohexene boat-to-boat inversions. However, fullerene derivatives **9**, **10**, **12** and **14** deviate from this trend line by approximately 2 kcal/mol. These four derivatives are the only ones that bear properly positioned phenyl rings such that they may engage in favorable CH– $\pi$  interactions with the fullerene cage. This additional CH– $\pi$  interaction disrupts the trend described by Martin.

## CONCLUSIONS

Several *o*-quinodimethane adducts of [60]fullerene were synthesized and studied using variable temperature NMR. Evaluation of the rate constants associated with the first-order transition states for cyclohexene boat-to-boat inversions enables quantification of  $\Delta G^\ddagger$  values for each inversion. The results are interpreted to indicate that *ortho* phenyl hydrogens on properly positioned phenyl substituents engage in stabilizing aryl CH–fullerene  $\pi$  interactions. These interactions contribute to the ground state stabilities of [60]fullerene–QDM adducts like derivatives **9**, **10**, **12** and **14**, thereby leading to unusually high barriers to cyclohexene boat-to-boat inversions compared to derivatives like **1–8** and **13** that do not enjoy similar CH– $\pi$  interactions. The difference in activation energies ( $\Delta G^\ddagger$ ) for boat-to-boat inversions of constitutional isomers **10** and **13** suggests a lower limit for an aryl CH–fullerene  $\pi$  interaction of approximately 0.95 kcal/mol.

## EXPERIMENTAL SECTION

**VT- $^1\text{H}$  NMR Spectroscopy.** Variable temperature  $^1\text{H}$  NMR spectra were collected on an FT-NMR operating at 499.763 MHz. Chemical shift values were reported in parts per million (ppm) relative to  $(\text{CH}_3)_4\text{Si}$  (TMS). The solvent used in all cases was *o*-dichlorobenzene- $d_4$ . Low temperature spectra were obtained with the use of a FTS cooling system.

**NMR Line-shape Analyses.** Dynamically broadened NMR spectra were simulated using WinDNMR.<sup>21</sup> All parameters except the rate-constant ( $k$ ) were taken from the slow-exchange spectra or near the slow-exchange limit and adjusted until the line-shapes matched. Subsequently,  $\Delta\nu$  was iterated until the simulated line-shape overlaid the spectrum. Iteration on both  $k$  and spectral amplitude was carried out sequentially until a best fit was achieved.

**Syntheses. Fullerene Adduct of 2,3-Bis(bromomethyl)-1,4-diphenylbenzene (**10**).** A 250 mL round bottomed flask was charged with [60]fullerene (0.300 g, 0.42 mmol) and toluene (125 mL). The mixture was stirred and purged with nitrogen for 10 min. A QDM precursor, 2,3-bis(bromomethyl)-1,4-diphenylbenzene (0.052 g, 0.12 mmol), potassium iodide (0.240 g, 1.44 mmol) and 18-crown-6 (0.420 g, 1.59 mmol) were added to the fullerene solution. The resulting mixture was boiled for 18 h in the dark under nitrogen. The cooled mixture was concentrated under reduced pressure. The crude solid was washed with chloroform until the filtrate ran clear. The chloroform solution was washed with water, concentrated under reduced pressure and purified via two column chromatography steps (silica, carbon disulfide eluent). The fullerene adduct was isolated as a brown powder with  $R_f = 0.65$  (0.072 g, 59%).  $^1\text{H}$  NMR (500 MHz, *o*-dichlorobenzene- $d_4$ )  $\delta$  4.52 (2H,  $J = 14$  Hz), 4.72 (2H,  $J = 14$  Hz), 7.29–7.33 (m, 2H), 7.41–7.46 (m, 4H), 7.52 (s, 2H), 7.53–7.57 (m, 4H);  $^{13}\text{C}$  NMR (125 MHz,  $\text{CS}_2/\text{CDCl}_3$ )  $\delta$  41.8, 65.8, 127.4, 128.5, 128.8, 129.5, 135.3, 135.9, 136.0, 140.1, 140.2, 140.5, 140.7, 141.6, 141.7, 142.0, 142.09, 142.11, 142.15, 142.5, 142.6, 143.06, 143.09, 144.7, 145.0, 145.32, 145.37, 145.44, 145.54, 145.6, 145.66, 145.71, 146.19, 146.23, 146.4, 147.6, 156.4, 156.5. LDI-MS  $m/z$  976, 977, 978. HRMS (ESI) calcd for  $\text{C}_{30}\text{H}_{17}$  ( $M + \text{H}$ ) 977.1325; found, 977.1303.

**5,6-Bis(bromomethyl)-4,7-diphenylisobenzofuran-1,3-dione (11).** A round bottomed flask was charged with 5,6-dimethyl-4,7-diphenylisobenzofuran-1,3-dione<sup>22</sup> (0.200 g, 0.61 mmol), *N*-bromosuccinimide (305 mg, 1.7 mmol), carbon tetrachloride (25 mL) and catalytic benzoyl peroxide. The mixture was boiled for 54 h. The cooled mixture was diluted with chloroform and washed several times with water. The organic layer was dried over calcium chloride and concentrated under reduced pressure to yield a sticky solid. The solids were triturated with hexanes affording the dibromide as a light yellow powder (260 mg, 88%). <sup>1</sup>H NMR (400 MHz, CDCl<sub>3</sub>) δ 4.58 (s, 4H), 7.39–7.46 (m, 4H), 7.54–7.59 (m, 6H); <sup>13</sup>C NMR (100 MHz, CDCl<sub>3</sub>) δ 26.0, 128.7, 128.9, 129.1, 129.6, 133.0, 142.9, 144.9, 160.8. HRMS (ESI) calcd for C<sub>22</sub>H<sub>14</sub><sup>79</sup>Br<sub>2</sub>NaO<sub>3</sub> (M + Na) 506.9202; found, 506.9216.

**Fullerene Adduct of 5,6-Bis(bromomethyl)-4,7-diphenylisobenzofuran-1,3-dione (12).** A nitrogen flushed round bottomed flask was charged with 5,6-bis-bromomethyl-4,7-diphenylisobenzofuran-1,3-dione (80 mg, 0.16 mmol), [60]fullerene (370 mg, 0.51 mmol), 18-crown-6 (725 mg, 2.7 mmol), potassium iodide (300 mg, 1.8 mmol) and toluene (150 mL). The resulting mixture was boiled under nitrogen in the dark for 14 h. The cooled mixture was washed successively with saturated aqueous sodium bisulfite and water. The organic layer was concentrated under reduced pressure. The crude brown solids were purified by flash column chromatography (silica) using carbon disulfide eluent to remove unreacted [60]fullerene followed by carbon disulfide/dichloromethane (1:1, v/v) to afford the fullerene adduct as a brown solid with R<sub>f</sub> = 0.2 (55 mg, 32%). <sup>1</sup>H NMR (400 MHz, CS<sub>2</sub>/CDCl<sub>3</sub>) δ 4.67 (2H, J = 14.2 Hz), 4.55 (2H, J = 14.2 Hz), 7.19–7.23 (m, 2H), 7.37–7.43 (m, 2H), 7.47–7.54 (m, 5H), 7.57–7.62 (m, 2H); <sup>13</sup>C NMR (100 MHz, CS<sub>2</sub>/CDCl<sub>3</sub>) δ 41.9, 65.2, 127.9, 128.7, 128.8, 129.1, 129.4, 133.5, 135.5, 140.29, 140.30, 140.5, 141.8, 142.0, 142.2, 142.7, 142.8, 143.2, 144.5, 144.7, 145.3, 145.6, 145.7, 146.2, 146.4, 146.6, 147.8, 155.0, 155.3, 161.4. LDI-MS m/z 1046, 1047, 1048. HRMS (ESI) calcd for C<sub>82</sub>H<sub>14</sub>NaO<sub>3</sub> (M + Na) 1069.0835; found, 1069.0836.

**Fullerene Adduct of 4,5-Bis(bromomethyl)-1,2-diphenylbenzene (13).** A 200 mL round bottomed flask was charged with [60]fullerene (0.300 g, 0.42 mmol), 4,5-bis(bromomethyl)-1,2-diphenylbenzene, **15** (see below), (0.050 g, 0.12 mmol) and toluene (125 mL). Nitrogen was bubbled through the stirred mixture for 10 min. Potassium iodide (0.240 g, 1.44 mmol) and 18-crown-6 (0.570 g, 2.2 mmol) were added. The reaction mixture was boiled for 16 h in the dark under nitrogen. The cooled mixture was concentrated under reduced pressure. The crude solid was washed with chloroform until the filtrate ran clear. The combined filtrate was concentrated and purified via two column chromatography steps (silica, carbon disulfide eluent). The fullerene adduct was isolated as a brown powder with R<sub>f</sub> = 0.6 (0.075 g, 64%). <sup>1</sup>H NMR (500 MHz, *o*-dichlorobenzene-*d*<sub>4</sub>) δ 4.42–4.54 (br, 2H), 4.77–4.90 (br, 2H), 7.14–7.22 (m, 6H), 7.30–7.34 (m, 4H), 7.76 (s, 2H); <sup>13</sup>C NMR (125 MHz, CS<sub>2</sub>/CDCl<sub>3</sub>) δ 45.1, 65.9, 126.8, 127.2, 127.6, 128.2, 129.1, 130.2, 135.4 (br), 136.6 (br), 137.3, 140.4 (br), 141.3, 141.7 (br), 141.9 (br), 142.2, 142.3, 142.7, 143.19, 143.27 (br), 144.8, 145.3 (br), 145.6 (br), 145.7 (br), 145.9, 146.4 (br), 146.6, 147.8, 156.6 (br), 156.9 (br). LDI-MS m/z 976, 977, 978. HRMS (ESI) calcd for C<sub>80</sub>H<sub>16</sub> (M) 976.1241; found, 976.1257.

**Fullerene Adduct of 5,6-Bis(bromomethyl)-1,2,3,4-tetraphenylbenzene (14).** A 200 mL round bottomed flask was charged with [60]fullerene (0.210 g, 0.29 mmol), 5,6-bis(bromomethyl)-1,2,3,4-tetraphenylbenzene (0.054 g, 0.095 mmol) and toluene (100 mL). The stirred mixture was purged with nitrogen for 10 min. Potassium iodide (0.162 g, 0.98 mmol) and 18-crown-6 (0.320 g, 1.21 mmol) were added to the fullerene solution. The resulting mixture was boiled for 17 h in the dark under nitrogen. The cooled mixture was concentrated under reduced pressure. The crude solids were washed with chloroform until the filtrate ran clear. The chloroform filtrate was washed successively with saturated aqueous sodium bisulfite and water and concentrated under reduced pressure. These solids were purified by column chromatography (silica, CS<sub>2</sub> eluent) to yield the fullerene adduct as a brown solid with R<sub>f</sub> = 0.5 (0.038 g, 36%). <sup>1</sup>H NMR (500 MHz, *o*-dichlorobenzene-*d*<sub>4</sub>) δ 4.51 (2H, J = 14 Hz), 4.61 (2H, J = 14

Hz), 6.70–6.75 (m, 2H), 6.78–6.85 (m, 2H), 6.88–6.95 (m, 2H), 6.98–7.04 (m, 2H), 7.06–7.13 (m, 4H), 7.16–7.22 (m, 2H), 7.23–7.30 (m, 4H), 7.44–7.50 (m, 2H); <sup>13</sup>C NMR (125 MHz, CS<sub>2</sub>/CDCl<sub>3</sub>) δ 42.6, 65.9, 125.5, 126.6, 126.7, 126.8, 127.8, 130.2, 130.7, 131.2, 135.3, 135.6, 136.1, 139.4, 140.0, 140.2, 140.3, 141.7, 141.8, 142.0, 142.14, 142.19, 142.23, 142.6, 143.13, 143.18, 144.7, 144.8, 145.1, 145.4, 145.5, 145.6, 145.8, 146.3, 146.5, 147.6, 156.5, 157.0. LDI-MS m/z 1129, 1130, 1131. HRMS (ESI) calcd for C<sub>92</sub>H<sub>24</sub>Na (M + Na) 1151.1770; found, 1151.1809.

**4,5-Bis(bromomethyl)-1,2-diphenylbenzene (15).** Following a procedure adapted from Amijs and co-workers,<sup>23</sup> a 10 mL closed vessel microwave tube was charged with 4,5-dimethylbenzene (0.1 g, 0.39 mmol) and methyl acetate (3 mL) and a magnetic stirrer. *N*-Bromosuccinimide (0.15 g, 0.89 mmol) and a catalytic amount of AIBN were added to the solution. The mixture was heated in a CEM Discover microwave to 112 °C over 3 min. The mixture was held at this temperature for an additional 10 min. The cooled mixture was concentrated under reduced pressure to yield an orange oil. The crude oil was purified via column chromatography (silica, dichloromethane eluent). A sticky solid with R<sub>f</sub> = 0.8 was triturated with hexanes to yield 4,5-bis(bromomethyl)-1,2-diphenylbenzene as a white powder (0.11 g, 66%). <sup>1</sup>H NMR (400 MHz, CDCl<sub>3</sub>) δ 4.74 (s, 4H), 7.10–7.14 (m, 4H), 7.21–7.24 (m, 6H), 7.43 (s, 2H); <sup>13</sup>C NMR (100 MHz, CDCl<sub>3</sub>) δ 30.0, 127.2, 128.2, 129.8, 133.5, 135.7, 140.2, 141.8. HRMS (EI) calcd for C<sub>20</sub>H<sub>17</sub><sup>79</sup>Br (M + H - Br) 336.0514; found, 336.0515.

## ■ ASSOCIATED CONTENT

### ■ Supporting Information

Select variable temperature <sup>1</sup>H NMR spectra for **10**, **13** and **14**; room temperature <sup>1</sup>H NMR, <sup>13</sup>C NMR and LDI-MS spectra for compounds **10**–**15**. This material is available free of charge via the Internet at <http://pubs.acs.org>.

## ■ AUTHOR INFORMATION

### Corresponding Author

\*glen.miller@unh.edu

## ■ ACKNOWLEDGMENTS

We thank the National Science Foundation for generous support through the Nanoscale Science & Engineering Center for High-rate Nanomanufacturing (NSF EEC 0832785) and the New Hampshire EPSCoR Research Infrastructure Improvement award (NSF EPS 0701730).

## ■ REFERENCES

- (1) Nishio, M. *CrystEngComm* **2004**, *6*, 130–158.
- (2) (a) Tamres, M. *J. Am. Chem. Soc.* **1952**, *74*, 3375. (b) Reeves, L. W.; Schneider, W. G. *Can. J. Chem.* **1957**, *35*, 251.
- (3) Nishio, M.; Hirota, M.; Umezawa, Y. *The CH/π Interaction: Evidence, Nature, and Consequences*; Wiley-VCH: New York, 1998.
- (4) (a) Shibasaki, K.; Fujii, A.; Mikami, N.; Tsuzuki, S. *J. Phys. Chem. A* **2006**, *110*, 4397. (b) Morita, S.; Fujii, A.; Mikami, N.; Tsuzuki, S. *J. Phys. Chem. A* **2006**, *110*, 10583.
- (5) Cox, E. G.; Cruickshank, D. W. J.; Smith, J. A. S. *Proc. R. Soc.* **1958**, *A247*, 1.
- (6) Nakagawa, N.; Fujiwara, S. *Bull. Chem. Soc. Jpn.* **1961**, *34*, 143.
- (7) Suezawa, H.; Yoshida, T.; Ishihara, S.; Umezawa, Y.; Nishio, M. *CrystEngComm* **2003**, *5*, 514–18.
- (8) Olmstead, M. M.; Costa, D. A.; Maitra, K.; Noll, B. C.; Phillips, S. L.; van Calcar, P. M.; Balch, A. L. *J. Am. Chem. Soc.* **1999**, *121*, 7090.
- (9) Kroto, H. W.; Heath, J. R.; O'Brien, S. C.; Curl, R. F.; Smalley, R. E. *Nature* **1985**, *107*, 7779–7780.
- (10) Kratschmer, W.; Lamb, L. D.; Fostiropoulos, K.; Huffman, D. R. *Nature* **1990**, *347*, 354–358.
- (11) Taylor, R. *Lecture Notes on Fullerene Chemistry*; Imperial College Press: London, 1999; pp 268.

- (12) Belik, P.; Gugel, A.; Spickermann, J.; Mullen, K. *Angew. Chem., Int. Ed. Engl.* **1993**, *32* (1), 78–80.
- (13) Rubin, Y.; Khan, S.; Freedberg, D. I.; Yeretizian, C. *J. Am. Chem. Soc.* **1993**, *115*, 344–345.
- (14) Kost, D.; Carlson, E. H.; Raban, M. *Chem. Commun.* **1971**, 656.
- (15) Zhang, X.; Foote, C. S. *J. Org. Chem.* **1994**, *59*, 5235–5238.
- (16) Tago, T.; Minowa, T.; Okada, Y.; Nishimura, J. *Tetrahedron Lett.* **1993**, *34* (52), 8461–8464.
- (17) Nakamura, Y.; Minowa, T.; Tobita, S.; Shizuka, H.; Nishimura, J. *J. Chem. Soc., Perkin Trans. 2* **1995**, *12*, 2351–2357.
- (18) Illescas, B. M.; Martin, N.; Seoane, C. *J. Org. Chem.* **1997**, *62*, 7585–7591.
- (19) Gonzalez, B.; Herrera, A.; Illescas, B.; Martin, N.; Martinez, R.; Moreno, F.; Sanchez, L.; Sanchez, A. *J. Org. Chem.* **1998**, *63*, 6807–6813. See also: Herrera, A.; Martínez-Alvarez, R.; Martín, N.; Chioua, M.; Chioua, R.; Molero, D.; Sánchez-Vázquez, A.; Almy, J. *Tetrahedron* **2009**, *65*, 5817–5823.
- (20) (a) Bredow, K.; Jaeschke, A.; Schmid, H.; Friebolin, H.; Kabuss, S. *Org. Magn. Reson.* **1970**, *2*, 543–555. (b) Briggs, J. B.; Jazdyk, M. D.; Miller, G. P. *Acta Cryst. E* **2010**, *6* (1), o12.
- (21) Reich, H. J. WinDNMR: Dynamic NMR Spectra for Windows *Journal of Chemical Education Software* **3D2**.
- (22) Chardonens, L.; Bitsch, S. *Helv. Chim. Acta* **1972**, *55*, 1345–1352.
- (23) Amijs, C. H. M.; Klink, G. P. M. v.; Koten, G. v. *Green Chem.* **2003**, *5*, 470–474.